Bull. Mater. Sci. (2022)45:56
https://doi.org/10.1007/s12034-021-02643-8

Effect of the O vacancy defects on the electronic structure and absorption spectra of BiOCl photocatalyst

KONG BO[1,2,*] and AN XINYOU[1]

[1] School of Physics and Astronomy, China West Normal University, Nanchong 637002, China
[2] School of Physics and Electronic Sciences, Guizhou Education University, Guiyang 550018, China
*Author for correspondence (xihuakb@yeah.net)

MS received 24 July 2021; accepted 23 November 2021

Abstract. In this study, the effects of the O vacancy defects with different charge states on the electronic structure and absorption spectra of bulk BiOCl are investigated using hybrid functional calculations. The previous calculations have shown that the O vacancy defects in BiOCl only could present the neutral (V_O^0) and +2 charge (V_O^{2+}) states. In the present study, it is first found and affirmed that the V_O^{2+} defect in BiOCl acts as an electron capture centre, and the direct recombination of the photogenerated electron–hole pairs can be effectively inhibited by the V_O^{2+} defect. While the V_O^0 defect acts as a recombination centre of the photogenerated carriers, it also induces a strong absorption peak around 500 nm in BiOCl. Moreover, the absorption strengthens with increasing O vacancy concentration. Therefore, it is suggested that BiOCl could present more significant photocatalytic activity via controlling and optimizing the concentration ratio of oxygen vacancies in 0 and +2 charge states. With an optimized concentration ratio, the photocatalytic activity of BiOCl should increase with increasing total O vacancy concentration in a larger concentration range. Our study thus provides a guideline or a reference for the design of highly efficient BiOCl or BiOCl-based photocatalyst with oxygen vacancies.

Keywords. BiOCl photocatalyst; oxygen vacancy defects V_O^0 and V_O^{2+}; electronic structures; optical absorption spectrum; photocatalytic activity.

1. Introduction

Bismuth oxychloride (BiOCl), as a novel photocatalyst, has attracted a great deal of attention in the environmental field because of its typical layered structure with a self-built internal static electric field along [001] direction, which highly favours the separation of the photo-induced charge carriers [1–3]. However, BiOCl has a wide bandgap (~3.5 eV) and only absorbs the UV (ultraviolet) light that accounts for less than 5% of sunlight energy [4]. At the same time, the separation efficiency of the photogenerated electron and hole pairs also need further enhancement. Therefore, many methods (including morphological control [5], constructing heterojunction [6], extrinsic doping [7], metal loading [8], defect engineering [9–17] as well as surface modification [9,11]) have been tried to enhance the visible-light absorption of BiOCl and accelerate the separation of the photogenerated electron–hole pairs. For these methods, defect engineering is a popular and promising method in enhancing the photocatalytic activity of BiOCl [13].

In defect engineering, it is known that oxygen vacancy is one of the fundamental and intrinsic defects in oxide semiconductor materials or semiconductor materials containing O elements, such as TiO_2, ZnO. It often gives a decisive or noticeable impact on their physicochemical properties, such as the electronic band structures, optical absorption, even chemical reactions and electron–hole pairs' separation [14]. In BiOCl, several exclusive experimental studies about the effects of oxygen vacancies on photocatalytic activity have been carried out. Firstly, in 2011, Ye *et al* [15] experimentally reported that oxygen vacancy plays a critical role in the photocatalytic degradation reaction of BiOCl. Plenty of oxygen vacancies under UV light irradiation improve the photogenerated electron–hole pairs' separation efficiency and, consequently, enhance the photocatalytic activity of BiOCl. They suggested that an oxygen vacancy defect state should exist near the bottom of the conduction bands. Thus, the electrons that are excited up to the conduction band (CB) of BiOCl under UV light irradiation, preferably transfer to the oxygen vacancy states rather than recombine with the photo-induced holes. Further, the recombination effect of the photogenerated electron and hole pairs is suppressed. In 2017, Zhang *et al* [16] synthesized BiOCl nanosheets via a modified solvothermal method, in which oxygen vacancies were produced using the electro-reduced method in a three-electrode cell with a platinum counter electrode. They showed that BiOCl with

Published online: 19 March 2022

oxygen vacancies presents superior photocatalytic activity, in contrast to the perfect one. Moreover, the experiments by Ye *et al* and Zhang *et al* showed or implied that the photocatalytic activity of BiOCl increases with increasing oxygen vacancy concentration. However, in 2018, Cai *et al* [17] synthesized BiOCl nanosheets with oxygen vacancies via the solvothermal method, in which the concentration of xylitol controlled the concentration of oxygen vacancies. They showed that the photocatalytic activity of the as-prepared sample increases with increasing oxygen vacancy concentration and then decreases after an optimum oxygen vacancy concentration. In addition, BiOCl-based heterojunctions with oxygen vacancies also present enhanced photocatalytic activity, in contrast to that without oxygen vacancies in experiments [18,19]. Therefore, oxygen vacancies in BiOCl or BiOCl-based photocatalysis have very important effects on improving their photocatalytic activities. However, the corresponding microscopic mechanisms are unconfirmed or promiscuous in both experiments and theory. In theory, although the effects of oxygen vacancy on the electronic and optical, further photocatalytic properties of BiOCl have been studied using first-principles calculations [14,20,21]; nevertheless, unfortunately, these calculations only focused on the neutral charge state of oxygen vacancy. In contrast, oxygen vacancy in other charge states in BiOCl could exist [22] under the thermal equilibrium growth conditions or with the extrinsic means, such as the electrical means, and could have important effects on the photocatalytic properties of BiOCl. At the same time, these calculations also cannot reasonably explain or support Ye *et al*'s suggestion about the mechanism of the improved BiOCl photocatalytic activity with the presentation or creation of oxygen vacancies [15]. Also, the contradiction between Zhang *et al*'s [16] experiment and Cai *et al*'s [17] experiment is not understood. On the other hand, the effects of other native defects on the photocatalytic properties of bulk BiOCl are also rarely investigated and reported. For our best knowledge, only Guan *et al* [11] experimentally reported that the predominant defects change from isolated vacancy defects V_{Bi}^{3-} (Bi vacancy in –3 charge state) to triple vacancy associates $V_{Bi}^{3-}V_O^{2+}V_{Bi}^{3-}$, as the thickness of the nanosheets reduces to the atomic scale. Moreover, they pointed out that the triple vacancy associates $V_{Bi}^{3-}V_O^{2+}V_{Bi}^{3-}$ should be responsible for the improvement of the photocatalytic activity in ultrathin BiOCl nanosheets. However, how the vacancy defects V_{Bi}^{3-} in bulk BiOCl affect the photocatalytic activity are not reported.

In our recent work [22], we systemically explored the origins of the native *p*-type conductivity and *n*-type conductivity in BiOCl using the screened hybrid functional calculations. We found that one or two defects from three vacancy defects V_{Bi}, V_O, V_{Cl} and the antisite defect O_{Cl} are the major intrinsic defects in BiOCl under the different growth conditions. (i) Under the O-rich (Bi-poor and Cl-poor) growth conditions, the antisite defects O_{Cl}^{1-} as the shallow acceptors are dominant, the intrinsic *p*-type conductivity in BiOCl under the high oxygen partial pressure or in the oxygen-saturated solutions primarily originates from the contributions of the antisite defects O_{Cl}^{1-}. (ii) Under the Bi-rich (O-poor and Cl-poor) growth conditions, the vacancy defects V_{Cl}^{1+} as the shallow donors are the major defects and are responsible for the *n*-type conductivity character of BiOCl. Particularly, under the growth conditions, whether the oxygen vacancy defects have contributions for the *n*-type conductivity were analysed and discussed in our previous work. We found that although the oxygen vacancy defect could have the lower formation energy and the higher concentration under a certain Bi-rich growth conditions, its transitional level from +2 to 0 charge states (only the +2 and 0 valance states are presented in the whole Fermi energy range) is deep. The oxygen vacancy is not a suitable donor. However, the measurements of the photocurrent or other extrinsic effects could lead to the production and ionization of the O vacancies, which could contribute to the *n*-type conductivity in BiOCl. (iii) Under the Cl-rich (Bi-poor and O-poor) growth conditions, the donor defects V_{Cl}^{1+} and the acceptor defects V_{Bi}^{3-} are the major defects and they compensate each other. However, in the theoretical work [22], how these major intrinsic defects affect the electronic and optical properties of bulk BiOCl, further affect the photocatalytic activity, were not mentioned and illustrated.

Therefore, the present work will systematically investigate the effects of the four major native defects, including three vacancy defects (V_{Bi}, V_O and V_{Cl}) and the antisite defect O_{Cl}, especially for the O vacancy defects V_O in the different charge states on the electronic structure and absorption spectra of bulk BiOCl using first-principle calculations. Further, their effects on the photocatalytic activities of BiOCl are discussed. It is found that the O vacancy defects V_O both in the neutral charge state V_O^0 and +2 charge state V_O^{2+} have significant effects on the electronic and optical properties of BiOCl, while other major defects have negligible effects. To some extent, why the oxygen vacancies in BiOCl or BiOCl-based photocatalysis in experiments were usually mentioned while other native defects were rarely reported [14–19] are further understood via the theoretical work.

2. Computational methodology

All calculations are performed using the Vienna *ab initio* simulation package (VASP) [23], with the projector augmented wave (PAW) approach. The generalized gradient approximation of Perdew *et al* [24] was used for geometrical optimization. The cutoff energy for basic functions is 550 eV. The crystal structure of BiOCl is a known tetragonal structure with six atoms in the unit cell. To discuss the effects of the vacancy and antisite defects, a $3 \times 3 \times 2$ BiOCl supercell containing 108 (pure)/107(with a vacancy)

atoms are constructed. Three vacancy defect sites (V_{Bi}, V_O and V_{Cl}) and the antisite defect O_{Cl} site in the 3 × 3 × 2 BiOCl supercell are displayed in figure 1. Generally, these defects are close to the centre of the supercell. The *k*-point mesh 2 × 2 × 2 for 108/107-atom BiOCl supercell is used for energy convergence. The convergence threshold on energy is set as 1.0×10^{-6} eV per atom. Atomic positions of every geometrical structure are relaxed until all residual forces are smaller than 0.01 eV $Å^{-1}$, while the adopted experimental lattice constants and cell volumes keep constant. For the calculations of electronic structure and optical properties, the screened hybrid functional of Heyd, Scuseria and Ernzerhof (HSE) is adopted for a more accurate description [25]. The adopted HSE06 functional has a screening parameter $\omega = 0.2$ $Å^{-1}$ and a mixing parameter $\alpha = 0.26$ for the short-range Hartree-Fock exchange. With these parameters, the calculated bandgap of bulk BiOCl (~3.5 eV) is compared well with the experimental data (3.51 [4] or 3.46 eV [26]) and previous HSE theoretical results (3.6 eV) [27].

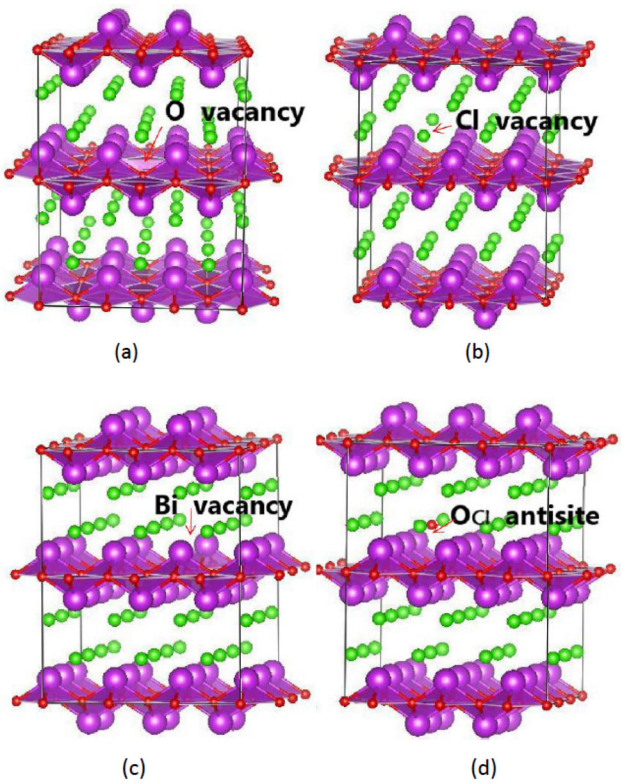

Figure 1. Three vacancy defect sites (**a**) V_O, (**b**) V_{Cl}, (**c**) V_{Bi} and the (**d**) antisite defect O_{Cl} site in a 3 × 3 × 2 BiOCl supercell. The red ball signs O atom, the green ball signs Cl atom and the purple ball signs Bi atom.

3. Results and discussions

3.1 *Effects of vacancy defects V_{Bi}, V_O and V_{Cl}, and antisite defect O_{Cl} on the crystal structure of BiOCl*

The optimized average Bi–O and Bi–Cl bond lengths in the perfect supercell and these around the defects are listed in table 1. It is seen that these major native defects in their neutral and dominant charged states mentioned in the introduction part (O vacancy in +2 charge state, Cl vacancy in +1 charge state, Bi vacancy in –3 charge state and O_{Cl} antisite in –1 charge state) in BiOCl mostly have the minor or negligible effects on the crystal structure except for the case of O vacancy in +2 charge state (V_O^{2+}). In the case of the V_O^{2+} defect, the obvious distortion is observed. The distance between the nearest two Bi atoms around O vacancy changes from 3.807 to 4.251 Å when the charge state changes from the neutral to +2 charge state. Therefore, it should not be easy for the formation of the V_O^{2+} defect. This is consistent with the calculations and analysis of the defect formation energy [22]. On the other hand, the Bi vacancy could be induced by the +2 charge state O vacancy and the triple vacancy associates $V_{Bi}^{3-}V_O^{2+}V_{Bi}^{3-}$ could present in ultrathin BiOCl nanosheets [11].

3.2 *Effects of vacancy defects V_{Bi}, V_O and V_{Cl}, and antisite defect O_{Cl} on the electronic structures and optical properties of BiOCl*

It is known that electronic structures can help us to understand many properties of the materials, such as optical properties. Firstly, the calculated band structure along the high symmetry direction, as well as the corresponding total density of states and projected density of states for pure BiOCl unit cell (tetragonal structure) using HSE06 hybrid functional, are presented in figure 2. It is seen that there is an indirect bandgap between the high symmetry Z point and R point. The bandgap value is about 3.5 eV. The corresponding projected density of states shows that the bottom

Table 1. Optimized average Bi–O and Bi–Cl bond lengths (Å) in the perfect supercell and these around the defects.

	Bi–O	Bi–Cl
Pure	2.327	3.056
V_O^0	2.324	3.051
V_O^{2+}	2.364	3.045
V_{Cl}^0	2.317	3.041
V_{Cl}^{1+}	2.316	3.060
V_{Bi}^0	2.311	3.061
V_{Bi}^{3-}	2.310	3.072
O_{Cl}^0	2.322	3.072
O_{Cl}^{1-}	2.337	3.033

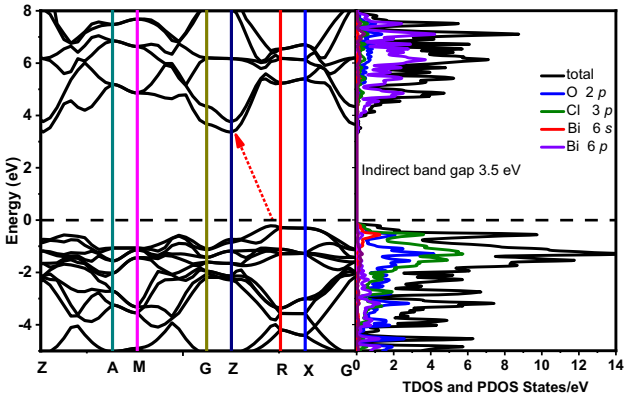

Figure 2. The calculated band structure, total density of states (TDOS) and projected density of states (PDOS) for pure BiOCl unit cell using HSE06. E_F is set to zero.

of the conduction bands is mainly composed of the Bi 6*p* orbitals, while the top of the valence bands mostly comes from the Cl 3*p* orbitals and O 2*p* orbitals. These are in good consistency with the experiments [26] and other hybrid functional calculations [27] mentioned in section 2.

Via the HSE calculations, the four kinds of major defects in BiOCl including three vacancy defects (V_O, V_{Bi} and V_{Cl}) and the antisite defect O_{Cl} in their neutral and dominant charged states on the effects of the electronic structures of BiOCl are shown in figure 3. It is found that the vacancy defect V_{Bi} and the antisite defect O_{Cl} in their neutral charge states make the Fermi energy level shift towards the valence bands and intersect with the valence bands. In contrast, the vacancy defects V_O and V_{Cl} make the Fermi energy level shift towards the conduction bands, and the Fermi energy level intersects with the conduction bands in the defect V_{Cl} case, compared to figure 2. This means that the vacancy defect V_{Bi} and the antisite defect O_{Cl} should be the acceptor and could contribute to the *p*-type conductivity, while the vacancy defects V_O and V_{Cl} should be the donors and could contribute to the *n*-type conductivity in BiOCl. These are consistent with the previous defect formation energy calculations and analysis [22]. Comparing figures 2 and 3, other few or significant changes for the band structure of BiOCl also occur because of these intrinsic defects. The fewer changes correspond to the vacancy defect V_{Cl} and the antisite defect O_{Cl}. The band structure of the supercell with one Cl vacancy defect or with one antisite defect O_{Cl} almost does not change in both the neutral charge state and the dominant charged state. Thus, the corresponding optical absorption spectrum also almost does not change, in contrast to the pure supercell case. This is one possible reason why there are no reports about the effects of the Cl vacancy defect and the antisite defect O_{Cl} on the physical properties of BiOCl in experiments for our knowledge, although they could form spontaneously under certain growth conditions because of the lower and negative formation energies [22].

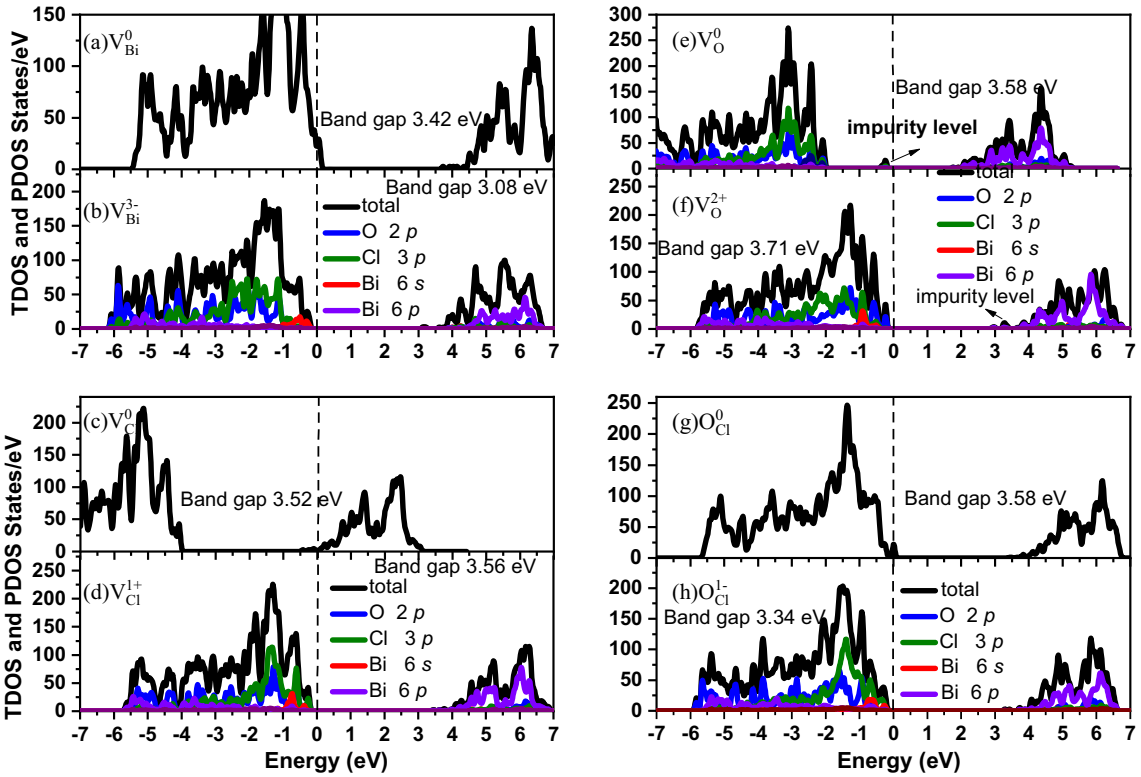

Figure 3. The calculated total density of states (TDOS) and projected density of states (PDOS) for four kinds of native defects in a 3 × 3 × 2 BiOCl supercell using HSE06. E_F is set to zero and is indicated by the dashed lines.

The more significant changes correspond to the Bi vacancy in the –3 charge state and the O vacancy in 0 and +2 charge states. The bandgap reduces to be 3.08 eV with the presence of the defect V_{Bi}^{3-} in BiOCl. However, the change is negligible in contrast to the case of BiOF [28], where the bandgap of BiOF supercell without and with the defect V_{Bi}^{3-} changes from 3.1 to 1.56 eV using the generalized gradient approximation calculations. The bandgap value 3.08 eV is still above the visible light region (1.65–2.75 eV). Simultaneously, there is no impurity level in the bandgap. Therefore, the defect V_{Bi}^{3-} in BiOCl almost does not change the optical absorption spectrum in the visible region in figure 4. However, obvious changes occur in the ultraviolet region. The redshift phenomenon is observed because of the decrease of the bandgap. Simultaneously, the absorption intensity in the region from 50 to 100 nm is significantly enhanced.

One can conclude that the Bi vacancies' presence benefits the improvement of the photocatalytic activity in BiOCl. However, in contrast to the O vacancy effects on the electronic structure and optical absorption spectrum of BiOCl, the Bi vacancy effects are weak. The experimental reports about the Bi vacancies' effects on the photocatalytic activity of BiOCl are also rare. One noticeable difference is that the impurity level is induced in the bandgap both in the neutral charge state and in the +2 charge state for the O vacancy case. The induced impurity level is apparent in the neutral charge state in figure 3e and is mainly composed of Cl 3*p* orbitals. Unfortunately, it is seen that the induced impurity level is close to the middle position of the bandgap and is a deep level. Thus, the neutral O vacancy in BiOCl could act as a recombination centre of the photogenerated electron–hole pairs, which is very harmful to improving the photocatalytic activity of BiOCl. On the other hand, there is a new and robust optical absorption peak around 500 nm, in figure 4, because of the presentation of the neutral O vacancy. Moreover, the absorption peak intensity in the visible light increases with increasing oxygen vacancy concentration via the comparison between the calculated optical spectrum in a 108/107 supercell (figure 4) and in a 48/47 atomic supercell (figure 5) without or with one O vacancy. This agrees with Ye *et al*'s experiments [15], where the new absorption peak around 468 nm becomes stronger with increasing oxygen vacancy concentration under UV light irradiation. However, the recombination centre effect induced by the neutral oxygen vacancy and the great enhancement of the optical absorption spectrum in the visible light region is the contrary two factors for improving the photocatalytic activity of BiOCl. It is not easy to judge which one is the primary factor in theory.

Surprisingly, the +2 charge state O vacancy effects on the electronic and optical properties of BiOCl are very different from those of the neutral charge state. In figure 3e and f, it is seen that the impurity level shifts towards the conduction band minimum when the charge state of the O vacancy changes from the neutral one to the +2 one. The impurity level induced by the defect V_O^{2+} is close to the conduction band minimum (the calculations of the band structure can more clearly present the fact). This is very significant for improving the photocatalytic activity of BiOCl. The electrons that are excited up to the conduction bands of BiOCl under UV light irradiation can be captured by the +2 charge state oxygen vacancies. Therefore, the photo-induced electrons on the conduction band minimum of BiOCl preferably transfer to the +2 charge state oxygen vacancies rather than recombine with the photo-induced holes. The direct recombination of the photo-induced charge carriers can be effectively inhibited by the +2 charge state oxygen vacancies in BiOCl. This is consistent with the suggested mechanism from the experiments [15]. Also, the decrease of the effective bandgap (about 2.98 eV) because of the presence of the O vacancy in the +2 charge state can make the optical absorption spectrum shift towards the low frequency. The absorption intensity in the region

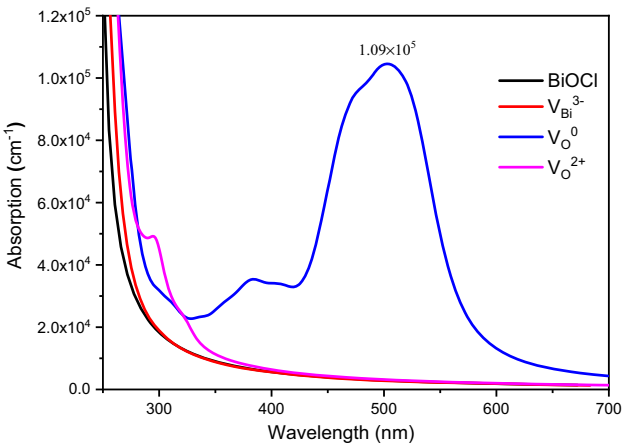

Figure 4. The calculated optical absorption spectrum for a 3 × 3 × 2 BiOCl supercell and V_{Bi}^{3-}, V_O^0 and V_O^{2+}, respectively, using HSE06 functional.

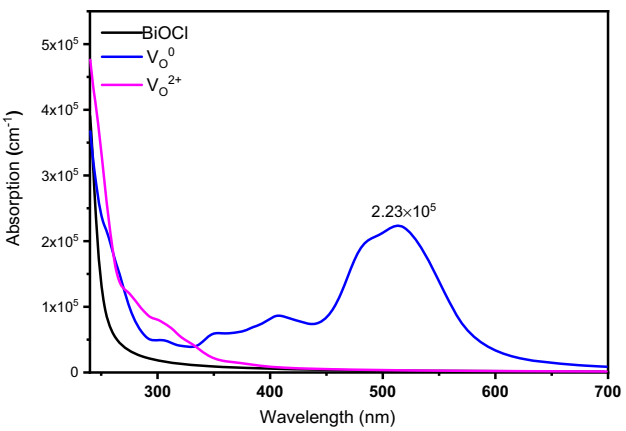

Figure 5. The calculated optical absorption spectrum for a 2 × 2 × 3 BiOCl supercell and the defects V_O^0 and V_O^{2+}, respectively, using HSE06 functional.

from 260 to 450 nm is enhanced evidently in figures 4 and 5. Thus, the O vacancies in the +2 charge state in BiOCl could greatly benefit the photocatalytic activity improvement, although the new absorption peak in the visible region disappears, the absorption intensity decreases significantly in the visible region, in contrast to the neutral O vacancy case. Nevertheless, the previous calculations and analysis of the defect formation energies [22] showed that the O vacancy concentration in the +2 charge state in BiOCl at any thermal equilibrium growth conditions should be very limited, because the transition level from 0 to +2 charge states is deep for the oxygen vacancy in BiOCl. At the same time, the neutral O vacancy concentration should be low in most thermal equilibrium growth environments in theory because of the positive and high formation energy. Therefore, to enhance the photocatalytic activity of BiOCl via the O vacancies, the productions of the rich O vacancies usually need extrinsic means in experiments [15–17]. Thus, in conjunction with Ye *et al*'s [15], Zhang *et al*'s [16] and Cai *et al*'s [17] experiments, we understand that the oxygen vacancies in BiOCl can be not only induced but also can be ionized partially with the artificial UV light irradiation [15] or the electro-reduced method [16]. Then, in Ye *et al*'s and Zhang *et al*'s experiments, the recombination centre effect from the neutral O vacancies is suppressed by the O vacancies in the +2 charge state. As a synergistic effect from the O vacancies in the 0 and +2 charge states, BiOCl displays superior photocatalytic activity. Moreover, the photocatalytic activity should increase with increasing oxygen vacancy concentration in a larger concentration range. While in Cai *et al*'s experiment [17], the UV light irradiation from the artificial light source or the electrical means is absent. The induced oxygen vacancies via the solvothermal method could mostly exist in the neutral charge state. When the concentration of oxygen vacancies was larger than a critical value, the recombination centre effect from the neutral oxygen vacancies should become stronger than the optical absorption spectrum's enhancement in the visible light region with increasing oxygen vacancy concentration. Therefore, Cai *et al*'s experiment showed that as-prepared samples have excellent photocatalytic activity under an optimum oxygen vacancy concentration and then decrease due to the increased oxygen vacancy concentration. Further, it is suggested that BiOCl could present the more significant photocatalytic activity via controlling and optimizing the concentration ratio of oxygen vacancies in the 0 and +2 charge states. With an optimized concentration ratio, the photocatalytic activity of BiOCl should increase with increasing total O vacancy concentration in a larger concentration range. For example, in Cai *et al*'s experiment [17], if the +2 charge state oxygen vacancy concentration could be increased, we believe that the optimum oxygen vacancy concentration could be enhanced, further, the better photocatalytic activity of BiOCl should be presented. Our study thus provides a guideline or a reference for the design of highly efficient BiOCl or BiOCl-based photocatalyst with oxygen vacancies.

4. Conclusions

In the study, the effects of the four major native defects including three vacancy defects (V_{Bi}, V_O and V_{Cl}) and the antisite defect O_{Cl}, especially for the O vacancy defects with different charge states on the electronic structure and absorption spectra of bulk BiOCl have been investigated using hybrid functional calculations. The calculations of electronic structures show that the intrinsic vacancy defect V_{Cl} and the antisite defect O_{Cl} both in the neutral and charged states almost do not affect the electronic and optical properties of BiOCl. This is one possible reason that the effect of the Cl vacancy defect or the antisite defect O_{Cl} on the physical properties of BiOCl is rarely reported in experiments, although they could form spontaneously under certain growth conditions because of the lower and negative formation energies. However, for the V_{Bi}^{3-}, V_O^{2+} and V_O^0 vacancy defects, their effects on the electronic and optical properties of BiOCl are apparent, especially for the O vacancy. The defect V_{Bi}^{3-} will decrease the bandgap of BiOCl from ~3.5 to 3.08 eV and make the optical absorption spectrum move towards the low frequency. The absorption intensity in the ultraviolet region from ~50 to ~100 nm is significantly enhanced. One can conclude that the Bi vacancies' presence benefits the improvement of the photocatalytic activity in BiOCl. However, in contrast to the O vacancy effects on the electronic structure and optical absorption spectrum of BiOCl, the Bi vacancy effects are weak.

The oxygen vacancy in the +2 charge state can induce a defect level lying near the photocatalyst's conduction band's bottom. The photo-induced electrons on the CB of BiOCl preferably transfer to oxygen vacancy states rather than recombine with the photo-induced holes. The direct recombination of photo-induced charge carriers can be effectively inhibited by the +2 charge state oxygen vacancies in BiOCl. While the neutral O vacancy makes a strong absorption peak appear around 500 nm in BiOCl, and the absorption intensity in the visible region is enhanced enormously. Moreover, it increases with increasing O vacancy concentration. However, the induced impurity level by the neutral O vacancy in BiOCl is close to the bandgap's middle position. It acts as the recombination centre of the photogenerated electron–hole pairs. In conjunction with experiments, it is understood that the artificial UV light irradiation or electrical means in experiments not only can induce the O vacancies but also can partially ionize the O variances. Then, the recombination centre effect from the neutral O vacancies is suppressed by the O vacancies in the +2 charge state. Further, the synergistic effects from the O vacancies in the 0 and +2 charge states make BiOCl display superior photocatalytic activity.

Therefore, it is suggested that BiOCl could present more significant photocatalytic activity by controlling and optimizing the concentration ratio of oxygen vacancies in the 0 and +2 charge states. With an optimized concentration ratio, the photocatalytic activity of BiOCl should increase with increasing total O vacancy concentration in a larger concentration range. Our study thus provides a guideline or a reference for the design of highly efficient BiOCl or BiOCl-based photocatalyst with oxygen vacancies.

Acknowledgements

This study was supported by the Doctor Research Fund of China West Normal University (Grants No. 412773) as well as the NSFC under Grant No. 11464005.

References

[1] Li H and Zhang L 2014 *Nanoscale* **6** 7805
[2] Malathy P, Vignesh K, Rajarajan M and Suganthi A 2014 *Ceram. Int.* **40** 101
[3] Kudo A, Omori K and Kato H 1999 *J. Am. Chem. Soc.* **121** 11459
[4] Wang W, Huang F and Lin X 2007 *Scripta Mater.* **56** 669
[5] Ding L, Wei R, Chen H, Hu J and Li J 2015 *Appl. Catal. B* **172–173** 91
[6] Jia X, Cao J, Lin H, Zhang M, Guo X and Chen S 2017 *Appl. Catal. B* **204** 505
[7] Yu J, Wei B, Zhu L, Gao H, Sun W and Xu L 2013 *Appl. Surf. Sci.* **284** 497
[8] Weng S, Chen B, Xie L, Zheng Z and Liu P 2013 *J. Mater. Chem. A* **1** 3068
[9] Ye L, Zan L, Tian L, Peng T and Zhang J 2011 *Chem. Commun.* **47** 6951
[10] Chen Z X J, Fang J W and Zhang S Y 2015 *Int. J. Thermophys.* **36** 910
[11] Guan M, Xiao C, Zhang J, Fan S, An R, Cheng Q *et al* 2013 *J. Am. Chem. Soc.* **135** 10411
[12] Fujishima Y, Okamoto S, Yoshiba M, Itoi T, Kawamura S, Yoshida Y *et al* 2015 *J. Am. Chem. Soc.* **3** 8389
[13] Liu X, Xu H, Li D, Zou Z and Xia D 2019 *ChemistrySelect* **4** 12245
[14] Zhang X, Zhao L, Fan C, Liang Z and Han B 2012 *Comp. Mater. Sci.* **61** 180
[15] Ye L, Zan L, Tian L, Peng T and Zhang J 2011 *Chem. Commun.* **47** 951
[16] Zhang P, Qiu Y, Yang S, Jiao Y, Ji C, Li Y *et al* 2017 *Mater. Res. Bull.* **96** 478
[17] Cai Y, Li D, Sun J, Chen M, Li Y, Zou Z *et al* 2018 *Appl. Surf. Sci.* **439** 697
[18] Wang Q, Wang W, Zhong L, Liu D, Cao X and Cui F 2018 *Appl. Catal. B* **220** 290
[19] Liu G, Xu H, Li D, Zou Z, Li Q and Xia D 2019 *EurJIC* **17** 4887
[20] Zhang H, Liu L and Zhou Z 2012 *Phys. Chem. Chem. Phys.* **14** 1286
[21] Jing T, Dai Y, Ma X, Wei W and Huang B 2016 *Phys. Chem. Chem. Phys.* **18** 7261
[22] Kong B, Zeng T X and Wang W 2021 *Phys. Chem. Chem. Phys.* **23** 19841
[23] Kresse G and Joubert D 1999 *Phys. Rev. B* **59** 1758
[24] Perdew J P, Burke K and Ernzerhof M 1996 *Phys. Rev. Lett.* **77** 3865
[25] Heyd J, Scuseria G E and Ernzerhof M 2003 *J. Chem. Phys.* **118** 8207
[26] Zhang K L, Liu C M, Huang F Q, Zheng C and Wang W D 2016 *Appl. Catal. B* **68** 125
[27] Yao W, Zhang J, Wan Y and Ren F 2018 *Appl. Surf. Sci.* **435** 1351
[28] Yang Z, Pei Y, Tan S, Wang X, Liu L and Su X 2013 *Comp. Mater. Sci.* **74** 50